NATURAL NANOFLUID CONVECTION IN RECTANGULAR POROUS DOMAINS

Hamza Sayyou [*] , ***Jabrane Belabid*** , ***Karam Allali***

Laboratory of Mathematics, Computer Science and Applications, Faculty of Sciences and Technologies, University Hassan II of Casablanca, P.O. Box 146, Mohammedia 20650, Morocco

Abstract

In this paper, the free convective flow and heat transfer in a porous rectangular enclosures filled with Cu-water nanofluid is studied and analyzed. The cavity sidewalls are exposed to a constant heat flux and the horizontal walls are assumed to be adiabatic. The governing equations describing the problem are solved using a finite difference method. The main parameters of our problem are: aspect ratio, volume fraction of nanoparticles, types of media, porosity of the medium and Rayleigh number. The results indicate that an increase in aspect ratio from 0.1 to 0.7 leads to an exponential increase in the Nusselt number, which then reaches a maximum value. However, the heat transfer rate progressively decreases for aspect ratios above 0.7. Moreover, the addition of more Cu-nanoparticles weakens the heat transfer. As a result, when the porous medium has low thermal conductivity, the solid matrix porosity becomes particularly more effective in improving heat transfer.

Keywords: *Natural convection, Porous medium, Aspect ratio, Rectangular cavity, Nanofluid.*

1 Introduction

Natural convection is a fundamental mode of heat transfer that occurs when a fluid is heated and rises, displacing cooler fluid in the process. The phenomenon has been studied extensively due to its practical applications in various fields, including building design, electronics cooling, and renewable energy systems see the notable books Nield and Bejan [14], Vafai [25]. Recent studies have focused on the application of natural convection in microfluidics, such as microchannels, microreactors, and micro-heat exchangers. For instance, the study by Jung and Park [11] investigated the heat transfer enhancement of natural convection in a microchannel heat sink using Al_2O_3-water nanofluid. Another recent study by Sharifpur et al. [20] investigated the natural convection heat transfer performance in a cavity filled with TiO_2-water nanofluid. They found that the heat transfer rate attain the maximum for 0.05% nanoparticle volume fraction. Anwar et al. [3] performed a numerical study on convective flow in heat sinks of a mini-channel saturated with CuO-water nanofluid for microprocessor cooling.

Nanofluids are a type of fluid that contain suspended nanoparticles, typically less than 100 nm in size, in a base fluid. The addition of nanoparticles to the base fluid can significantly affect its thermal conductivity and convective heat transfer coefficient, leading to improved heat transfer rates. Nanofluids can be synthesized using various types of nanoparticles, such as metal oxides, carbides, nitrides, and carbon-based materials, and base fluids, such as water, ethylene glycol, and oil (see Keblinski et al. [12]). Nanofluids have been studied in various geometries and configurations (see Asmadi et al. [4],Rahimi et al. [16] and Sadeghi

[*]Corresponding author: hamzasayyou@gmail.com

et al. [19]), with researchers exploring their potential applications in heat exchangers, solar collectors, and cooling systems, among others. For example, the study by Xu et al. [26] investigated the thermal performance of a flat plat solar collector filled with $\mathrm{Al_2O_3}$-water nanofluid and found that the collector's efficiency is impacted by the nanoparticles. Another study by Alklaibi et al. [2] examined the heat transfer characteristics of a plate heat exchanger using MWCNT + $\mathrm{Fe_3O_4}$-water hybrid nanofluid. A study was conducted by Yao et al. [27] using the lattice Boltzmann method to investigate free convection heat transfer flow in a porous-partial cavity with the application of different kinds of nanoparticles (Al_2O_3, Cu, and S_iO_2).

One of the key parameters affecting natural convection is the aspect ratio of the cavity, which is the ratio of its length to its width. The aspect ratio can have a significant impact on the heat transfer characteristics of the system, affecting the flow patterns, temperature distribution, and heat transfer rate. Understanding the effect of aspect ratio is important for designing and optimizing heat transfer systems in various applications. Recent studies have explored the effect of aspect ratio on natural convection in various geometries, such as annular cavities (Belabid et al. [7]) and rectangular cavities (Oztop and Abu-Nada [15]). These studies highlight the importance of understanding the impact of aspect ratio on natural convection for various geometries and applications. Another recent study by Redouane et al. [18] investigated the natural convection in a porous triangular corrugated enclosure with a rotate centered cylindrical cavity filled with Ag-MgO/water hybrid nanofluid .

This article examines how the aspect ratio and other parameters affect natural convection in a rectangular cavity filled with a copper/water nanofluid. Our aim is to analyze the heat transfer characteristics of the physical system and determine how the aspect ratio impacts the convective heat transfer rate. In this analysis we adopt the mathematical model of Tiwari and Das [24], and it builds upon the existing literature on free convection in enclosures filled with nanofluids, it sheds light on the complex interplay between the geometry of the cavity and the properties of the nanofluid. The amount of studies conducted on the influence of aspect ratio on natural convection in cavities containing nanofluids is constrained, and our study fills this gap in the literature. The results of our study could have practical implications for the design and optimization of heat transfer systems in various applications, including electronics cooling, power generation and renewable energy systems.

2 Mathematical formulation of the Problem

The geometrical configuration and the chosen boundary conditions of the present study is illustrated in Fig. 1. Considering a two-dimensional saturated porous cavity of the height H and the width L such that the aspect ratio $Ar = H/L$ containing a Copper-water nanofluid. The enclosure heated constantly from the left side T_{hot} and the right one is cooled T_{cold}, while the top and bottom walls are thermally insulated $\partial\widetilde{T}\Big/\partial y = 0$. We admit that the porous medium in thermal equilibrium. The mixture is incompressible, Newtonian and flow pattern is laminar.

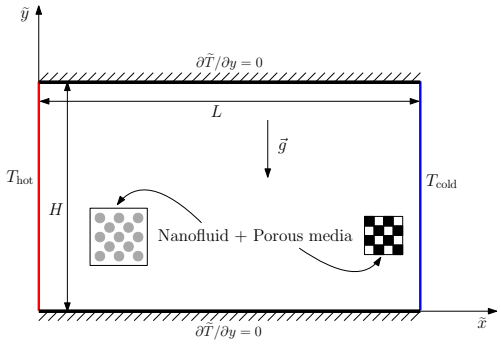

Figure 1: Sketch of the physical problem

2.1 The effective thermal physical parameters

All the thermophysical properties are supposed to be unchanged, except for density in the buoyancy term, depending on the Darcy-Boussinesq model. The porous matrix composed of the aluminium foam or the glass balls is homogeneous and isotropic. The thermal physical parameters of water, solid matrix and nano-size particles are cited in Tab. 1. The following thermal physical expressions have been noticed in Abu-Nada and Oztop [1], see also Haddad et al. [10]

Table 1: The base fluid, the nanoparticles and the solid structure thermophysical properties (see Sheremet et al. [21]).

Physical properties	Clear fluid (water)	Cu	Aluminium foam	Glass balls
$C_p\left[\mathrm{J}\cdot\mathrm{kg}^{-1}\cdot\mathrm{K}^{-1}\right]$	4179	385	897	840
$\rho\left[\mathrm{kg}\cdot\mathrm{m}^{-3}\right]$	997.1	8933	2700	2700
$k\left[\mathrm{W}\cdot\mathrm{m}^{-1}\cdot\mathrm{K}^{-1}\right]$	0.613	400	205	1.05
$\beta\times10^{-5}\left[\mathrm{K}^{-1}\right]$	21	1.67	2.22	0.9

The heat capacitance of the nanofluid can be determined by:

$$(\rho \mathrm{C_p})_{\mathrm{nf}} = (1-\varphi)(\rho \mathrm{C_p})_{\mathrm{f}} + \varphi(\rho \mathrm{C_p})_{\mathrm{p}} \tag{1}$$

The thermal conductivity of the nanofluid represented by:

$$\mathrm{k_{nf}} = \mathrm{k_f}\left(\frac{\mathrm{k_p}+2\mathrm{k_f}-2\varphi\left(\mathrm{k_f}-\mathrm{k_p}\right)}{\mathrm{k_p}+2\mathrm{k_f}+\varphi\left(\mathrm{k_f}-\mathrm{k_p}\right)}\right) \tag{2}$$

The nanofluid viscosity approximated in function of base fluid viscosity expressed as:

$$\mu_{\mathrm{nf}} = \frac{\mu_{\mathrm{f}}}{(1-\varphi)^{2.5}} \tag{3}$$

The buoyancy coefficient of the nanofluid is:

$$(\rho\beta)_{\mathrm{nf}} = (1-\varphi)(\rho\beta)_{\mathrm{f}} + \varphi(\rho\beta)_{\mathrm{p}} \tag{4}$$

The heat capacitance of the medium is:

$$\left(\rho \mathrm{C_p}\right)_{\mathrm{m}} = \varepsilon\left(\rho \mathrm{C_p}\right)_{\mathrm{f}} + (1-\varepsilon)\left(\rho \mathrm{C_p}\right)_{\mathrm{s}} \tag{5}$$

More physical properties are shown as:

$$\mathrm{k_m} = \varepsilon \mathrm{k_f} + (1-\varepsilon)\mathrm{k_s} \tag{6}$$

The thermal conductivity of nanofluid saturated porous medium is:

$$\begin{aligned} \mathrm{k_{mnf}} &= \varepsilon \mathrm{k_{nf}} + (1-\varepsilon)\mathrm{k_s} \\ &= \varepsilon \mathrm{k_{nf}} + \mathrm{k_m} - \varepsilon \mathrm{k_f} \end{aligned} \tag{7}$$

2.2 Governing equations

Taking into consideration the above assumptions, the dimensional fluid flow and heat transfer equations are expressed as follow,

Continuity equation:

$$\boldsymbol{\nabla} \cdot \widetilde{\mathrm{V}} = 0 \tag{8}$$

Darcy law equation:

$$-\frac{\mu_{\mathrm{nf}}}{\mathrm{K}}\,\widetilde{\mathrm{V}} = \boldsymbol{\nabla}\widetilde{\mathrm{P}} + (\rho\beta)_{\mathrm{nf}}\,\mathbf{g}\,(\widetilde{\mathrm{T}} - \mathrm{T}_{\mathrm{cold}}) \tag{9}$$

Energy equation:

$$\big(\widetilde{\mathrm{V}} \cdot \boldsymbol{\nabla}\big)\widetilde{\mathrm{T}} = \frac{\mathrm{k}_{\mathrm{mnf}}}{(\rho \mathrm{C}_{\mathrm{p}})_{\mathrm{nf}}}\nabla^2\widetilde{\mathrm{T}} \tag{10}$$

Furthermore, we can introduce the following non-dimensional parameters as:

$$(x, y) = \left(\frac{\widetilde{x}}{L}, \frac{\widetilde{y}}{L}\right)\ ,\ u = \frac{\widetilde{u}\,(\rho C_p)_{\mathrm{nf}}}{k_{\mathrm{mnf}}},\ v = \frac{\widetilde{v}\,(\rho C_p)_{\mathrm{nf}}}{k_{\mathrm{mnf}}},\ \theta = \frac{\widetilde{T} - T_{\mathrm{cold}}}{T_{\mathrm{hot}} - T_{\mathrm{cold}}}.$$

The following non-dimensional velocity components defined such that:

$$V = (u, v) = \left(\frac{\partial \psi}{\partial y}, -\frac{\partial \psi}{\partial x}\right)$$

Moreover, the dimensionless stream-function temperature formulation obtained is:

$$\frac{\partial^2 \psi}{\partial x^2} + \frac{\partial^2 \psi}{\partial y^2} = Ra\,\frac{k_m}{k_{mnf}}\,\frac{(\rho C_p)_{nf}}{(\rho C_p)_f}\,\frac{\mu_f}{\mu_{nf}}\,\frac{(\rho\beta)_{nf}}{(\rho\beta)_f}\,\frac{\partial \theta}{\partial x} \tag{11}$$

$$\frac{\partial \psi}{\partial y}\,\frac{\partial \theta}{\partial x} - \frac{\partial \psi}{\partial y}\,\frac{\partial \theta}{\partial x} = \frac{\partial^2 \theta}{\partial x^2} + \frac{\partial^2 \theta}{\partial y^2} \tag{12}$$

where the Rayleigh number of the medium is

$$Ra = \frac{K\mathbf{g}H(\rho\beta)_f(\rho C_p)_f(T_{hot} - T_{cold})}{k_m \mu_f}$$

Besides, the non-dimensional boundary conditions associated to the dimensionless equations (11) and (12) are:

$$\begin{aligned} &\text{for } x = 0: \qquad \theta = 1 \quad \text{and} \quad \psi = 0 \\ &\text{for } x = 1: \qquad \theta = 0 \quad \text{and} \quad \psi = 0 \\ &\text{for } y = 0, Ar: \qquad \partial\theta/\partial y = 0 \quad \text{and} \quad \psi = 0 \end{aligned} \tag{13}$$

For a better analysis of the phenomenon, we had to measure the heat transfer ratio at the hot side using the local and average Nusselt number:

$$\mathrm{Nu} = \left(-\frac{k_{mnf}}{k_m}\right)\left.\frac{\partial \theta}{\partial x}\right|_{x=0} \qquad , \qquad \mathrm{Nu}_{\mathrm{avg}} = \frac{1}{Ar}\int_0^{Ar} Nu\,\mathrm{d}y \tag{14}$$

3 Numerical Methods

In this numerical study, a finite difference second order and accuracy scheme applied to solve the coupled equations (11) and (12) governed this problem corresponding to the boundary conditions (13). Those equations are descended from the equations of mass (8), momentum (9) and energy (10). The discretized algebraic linear system was calculated iteratively using Successive Under-Relaxation techniques. The convergence criterion for all dependent variables is less than 10^{-8}. As shown in Tab. 2, the code validations was carried out by comparing the mean Nusselt number $\mathrm{Nu}_{\mathrm{avg}}$ with some notable investigations.

Table 2: Comparison of the average Nusselt number with the previous works for $\varphi = 0$ (clear fluid) and square form $Ar = 1$.

Literature	Ra		
	10	100	1000
Bejan [6] (1979)	–	4.2	15.8
Gross et al. [9] (1986)	–	3.141	13.448
Manole and Lage [13] (1992)	–	3.118	13.637
Baytas and Pop [5] (1999)	1.079	3.16	14.06
Sun and Pop [23] (2014)	–	–	13.914
Sheremet et al. [21] (2015)	1.079	3.115	13.667
Sivasankaran et al. [22] (2019)	–	3.101	13.280
Rao and Barman [17] (2021)	–	3.146	13.576
This study	1.070	3.120	13.893

In addition, as depicted in Tab. 3 we were compare our calculation results with the presented work of Ghalambaz et al. [8].

Table 3: Comparison of the average Nusselt numbers with $\varphi = 0$, $\varepsilon = 0.9$ and $k_s = 2k_f$.

	$\mathrm{Ra} = 1000$	$Ar = 0.1$	$Ar = 10$
Our results	$\mathrm{Nu}_{\mathrm{avg}}$	1.723	5.146
Ghalambaz et al. [8]		1.667	5.083

Besides, a grid independency test was performed see Tab. 4, it permits us to select 250×250 mesh as the suitable for our coming analysis which is ensure a grid-independent solution.

Table 4: $\mathrm{Nu_{avg}}$ **variation for different grid size with** $Ra = 1000,\ Ar = 10,\ \varphi = 0.05$ **and** $\varepsilon = 0.8$ **(aluminium foam).**

Grid size (i × j)	$\mathrm{Nu_{avg}}$	$\Delta = \frac{\left\lvert \mathrm{Nu_{avg_{(i\times j)}}} - \mathrm{Nu_{avg_{(250\times 250)}}} \right\rvert}{\mathrm{Nu_{avg_{(i\times j)}}}} \times 100\%$
100×100	328.598	2.454%
150×150	323.893	1.037%
200×200	321.717	0.368%
250×250	320.532	–
300×300	319.818	0.223%
350×350	319.359	0.367%
400×400	319.049	0.464%

4 Results and Discussion

In this numerical investigation, the results are obtained for this following ranges of the governing parameters; the aspect ratio of the enclosure $(\mathrm{Ar} = 0.1 - 10)$, the nanoparticles volume fraction $(\varphi = 0 - 0.05)$, the porosity of the matrix $(\varepsilon = 0.3 - 0.8)$, the Rayleigh number $(\mathrm{Ra} = 10 - 1000)$. At last, we consider two types of solid matrix the glass balls and the aluminium foam.

Fig.2 shows the variation of the Nusselt average number with the aspect ratio for a base fluid. It is observed that the heat transfer boosts significantly for the range $0.1 \leq Ar \leq 0.7$. However, the Nusselt number tends to decrease gradually for $0.7 \leq Ar \leq 10$, It can also be seen that the Rayleigh number is a good parameter for managing the heat and flow improvement within the enclosure. Apparently, in Fig. 4 the porous matrix composition is negligible for a small aspect ratios. In contrast, it becomes more efficient with Ar up to 0.4. Also, Fig. 3 illustrates that for a given volume fraction, incrementing the porosity affect the heat transfer as previous for high values of aspect ratio, it is more pronounced with glass balls than aluminium foam solid matrices.

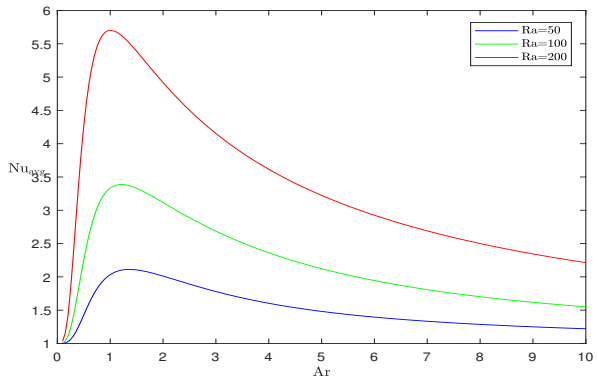

Figure 2: $\mathrm{Nu_{avg}}$ **vs Aspect ratio for a different values of Rayleigh number with** $\varphi = 0$

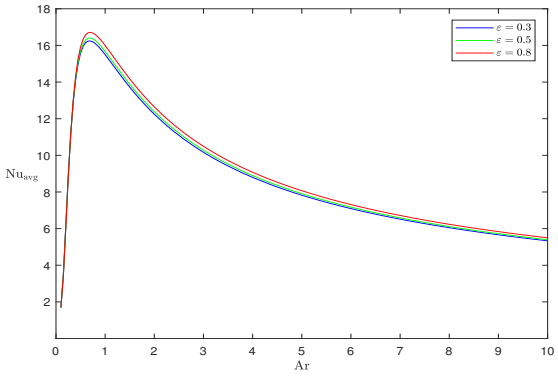

Figure 3: $\mathrm{Nu_{avg}}$ **vs Aspect ratio for different values of porosity taking** $\varphi = 0.05$ **and** $Ra = 1000$ **for the Glass Balls solid matrix**

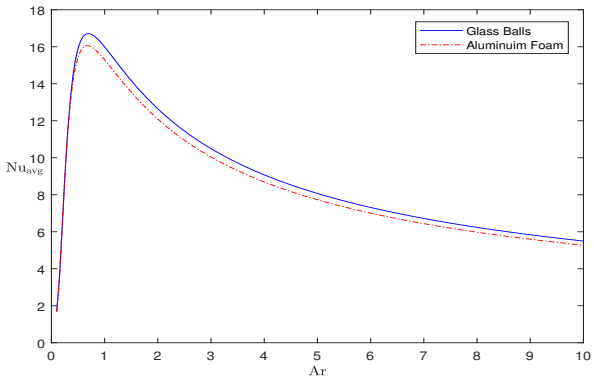

Figure 4: $\mathrm{Nu}_{\mathrm{avg}}$ **vs Aspect ratio for** $\varphi = 0.05$, $\varepsilon = 0.08$ **and** $Ra = 1000$ **for the two types of porous matrices**

Furthermore, in Fig. 5 we can see the variation of the temperature rate along the left wall $\mathrm{Nu}_{\mathrm{avg}}$ versus nanoparticles volume fraction φ using two types of porous media and three values of porosity. The results reveals that in case of the glass balls and for small Ar less than 0.35 the average Nusselt number raise with increasing of ε and it becomes the opposite behavior for Ar greater than the reflection value 0.35 and it is more remarkable in case of $Ar = 0.5$. Besides, for the aluminium foam the porosity doesn't change at all the $\mathrm{Nu}_{\mathrm{avg}}$. Moreover, adding more nanoparticles attenuate the heat transfer inside the cavity, in fact, the fluid with presence of the nanoparticles become more viscous. Essentially, for a high Rayleigh numbers the strength of the heat transfer is impacted by the effective viscosity and the thermal conductivity of the porous media.

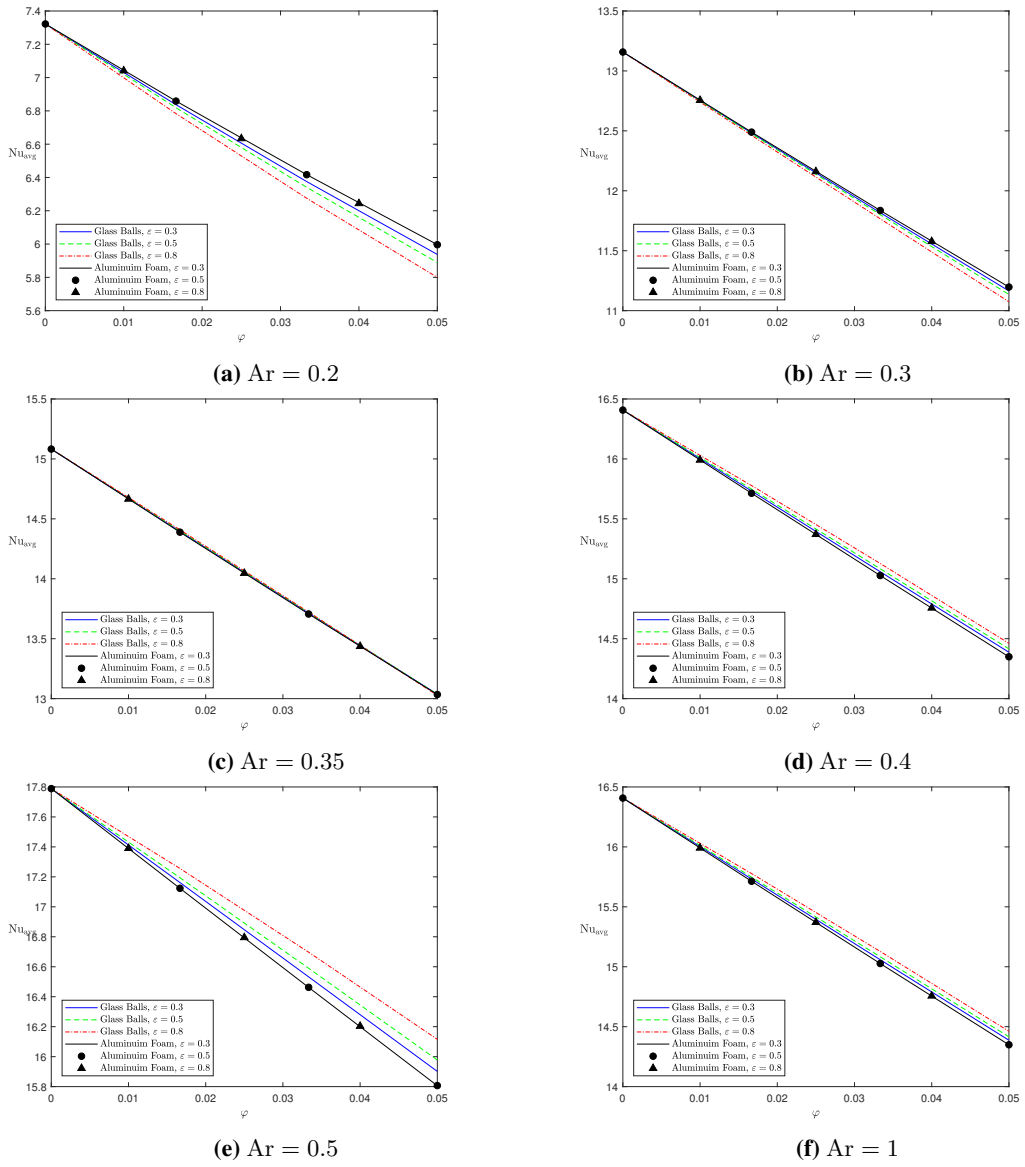

(a) Ar $= 0.2$ **(b)** Ar $= 0.3$

(c) Ar $= 0.35$ **(d)** Ar $= 0.4$

(e) Ar $= 0.5$ **(f)** Ar $= 1$

Figure 5: The influence of volume fraction φ on $\mathrm{Nu}_{\mathrm{avg}}$ for $Ra = 1000$ for different values of porosity and porous medium

Fig. 6 the results are presented in form of streamlines and isotherms for $0.1 \leq Ar \leq 1$. It is noticed that in case of very small aspect ratio $Ar = 0.1$ (a wide cavity) and for a high values of Ra the Nusselt average is small. The distribution of temperature is almost linear and we have a small circulation zone, it can be concluded that the heat is transferred by conduction throughout the enclosure. In addition, it's not worth mentioning that the porous structure has no important effect for the lowest aspect ratio. For the range $0.2 \leq Ar \leq 0.7$ the flow pattern is formed by a two flow circulations inside the cavity, it is owing to the temperature difference between the two walls, this formation remain visible with less thermal conductivity (glass balls).

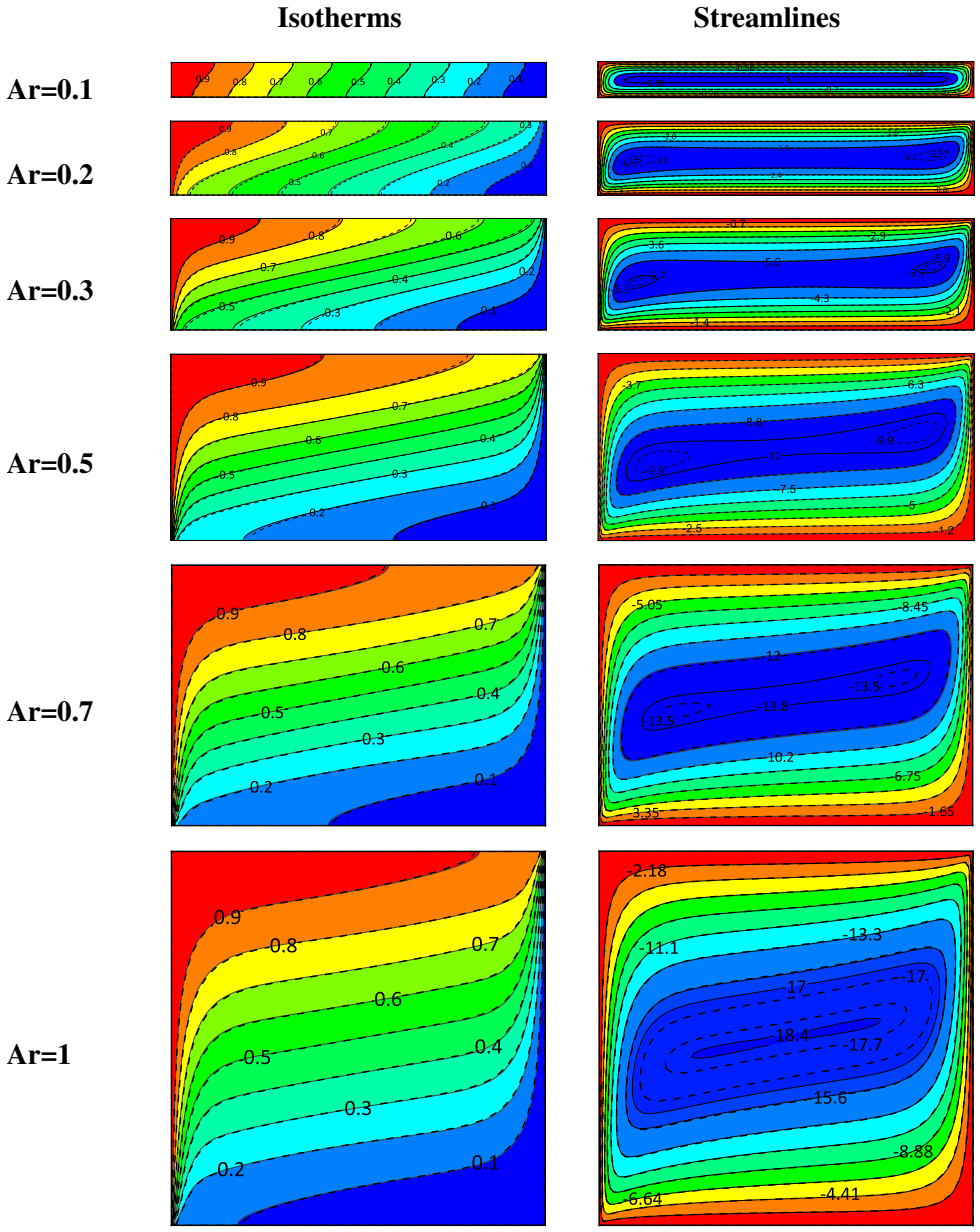

Figure 6: Isotherms and streamlines for $Ar = 0.1 - 1$ with glass balls (dashed lines) and aluminium foam (solid lines) solid matrices at $Ra = 1000$, $\varphi = 0.05$ and $\varepsilon = 0.5$

The obtained results in Fig. 7 are constituted by the contours of the temperature distribution and the flow pattern ranged the aspect ratio between 3 and 10. As much we increase Ar (a tall cavity) the flow stream is strengthened. Besides, near the top (i.e, bottom) insulated boundary a hot (i.e, cold) layer is formed, and the middle is thermally stratified. Eventually, the heat enhancement decreases slowly by incrementing Ar above 1.

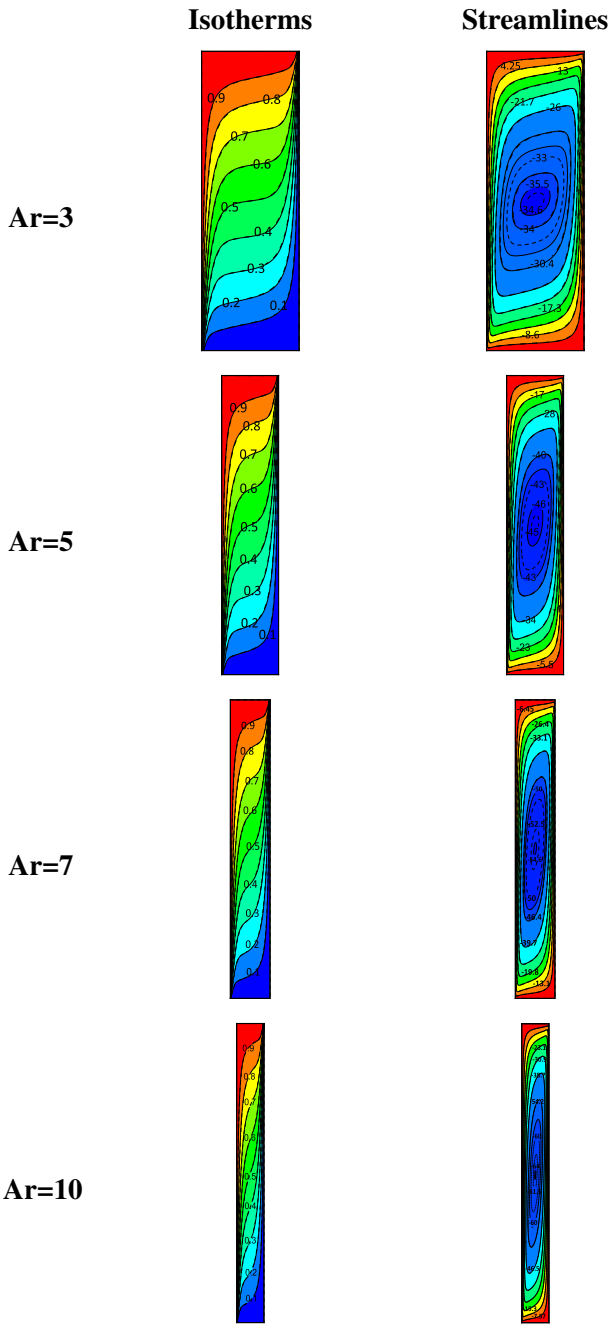

Figure 7: Isotherms and streamlines for $Ar = 3 - 10$ with glass balls (dashed lines) and aluminium foam (solid lines) solid matrices at $Ra = 1000$, $\varphi = 0.05$ and $\varepsilon = 0.5$

5 Conclusion

Free convection inside a porous saturated rectangular cavity filled with Cu-water nanofluid was numerically studied. the study has revealed some important findings regarding the impact of aspect ratio, the nanoparticles concentration, porosity and thermal conductivity of the porous media. The findings show that increasing

the aspect ratio leads to increase the flow stream inside the cavity. Moreover, adding more nanofluid particles deteriorate the heat enhancement. The main reason for the decline is primarily due to the increase in the dynamic viscosity caused by the existence of nanoparticles. In addition, as much as the thermal conductivity become considerable the effect of porosity is negligible. It is also observed that as the level of porosity in the porous material rises, there is typically a corresponding increase in the average Nusselt number.

Nomenclature

Latin symbols

$\mathbf{g}$ – Acceleration of the gravity $[\mathbf{m.s^{-2}}]$
$\mathbf{Nu}$ – Local Nusselt number
$\mathbf{Ra}$ – Rayleigh number of the porous medium
$\boldsymbol{Ar}$ – Aspect ratio
$\boldsymbol{C_p}$ – Specific heat at a constant pressure $[\mathbf{J.kg^{-1}.K^{-1}}]$
$\boldsymbol{H}$ – Hight of the cavity $[m]$
$\boldsymbol{K}$ – Permeability $[\mathbf{m^2}]$
$\boldsymbol{k}$ – Thermal conductivity $[\mathbf{W.m^{-1}.K^{-1}}]$
$\boldsymbol{L}$ – Width of the cavity $[m]$
$\boldsymbol{P}$ – Pressure $[\mathbf{Pa}]$
$\boldsymbol{T}$ – Temperature $[\mathbf{K}]$
$\boldsymbol{u, v}$ – Velocity components
$\boldsymbol{V}$ – Velocity vector $[\mathbf{m.s^{-1}}]$
$\boldsymbol{x, y}$ – Cartesian coordinates

Greek Symbols

$\boldsymbol{\alpha}$ – Thermal diffusivity $[\mathbf{m^2.s^{-1}}]$
$\boldsymbol{\beta}$ – Coefficient of thermal expansion $[\mathbf{K^{-1}}]$
$\boldsymbol{\mu}$ – Dynamic viscosity $[\mathbf{Pa.s}]$
$\boldsymbol{\phi}$ – Nanoparticles volume fraction
$\boldsymbol{\psi}$ – Dimensionless velocity
$\boldsymbol{\rho}$ – Density $[\mathbf{kg.m^{-3}}]$
$\boldsymbol{\theta}$ – Dimensionless temperature
$\boldsymbol{\varepsilon}$ – Porosity of the medium $[\mathbf{m^2}]$

Subscripts

avg – Average quatity
f – fluid
mnf – Nanofluid saturated with porous medium
m – Clear fluid saturated with porous medium
nf – Nanofluid
np – Nanoparticle
s – Solid matrix of the porous medium

Superscripts

$\sim$ – refers to dimensional variable

References

[1] E. Abu-Nada and H. F. Oztop. Effects of inclination angle on natural convection in enclosures filled with Cu–water nanofluid. *International Journal of Heat and Fluid Flow*, 30(4):669–678, Aug. 2009. ISSN 0142-727X. doi: 10.1016/j.ijheatfluidflow.2009.02.001. URL https://www.sciencedirect.com/science/article/pii/S0142727X0900023X.

[2] A. M. Alklaibi, L. S. Sundar, and K. V. V. Chandra Mouli. Experimental investigation on the performance of hybrid Fe3O4 coated MWCNT/Water nanofluid as a coolant of a Plate heat exchanger. *International Journal of Thermal Sciences*, 171:107249, Jan. 2022. ISSN 1290-0729. doi: 10.1016/j.ijthermalsci.2021.107249. URL https://www.sciencedirect.com/science/article/pii/S1290072921004105.

[3] M. Anwar, H. A. Tariq, A. A. Shoukat, H. M. Ali, and H. Ali. Numerical study for heat transfer enhancement using CuO water nanofluids through mini-channel heat sinks for microprocessor cool-

ing. *Thermal Science*, 24(5 Part A):2965–2976, 2020. URL https://www.doiserbia.nb.rs/Article.aspx?id=0354-98361900022A.

[4] M. S. Asmadi, Z. Siri, R. M. Kasmani, and H. Saleh. Nanoparticle shape effect on the natural-convection heat transfer of hybrid nanofluid inside a U-shaped enclosure. *Thermal Science*, 26 (1 Part B):463–475, 2022. URL https://www.doiserbia.nb.rs/Article.aspx?id=0354-98362100139A.

[5] A. C. Baytas and I. Pop. Free convection in oblique enclosures filled with a porous medium. *International Journal of Heat and Mass Transfer*, 42(6):1047–1057, Mar. 1999. ISSN 0017-9310. doi: 10.1016/S0017-9310(98)00208-7. URL https://www.sciencedirect.com/science/article/pii/S0017931098002087.

[6] A. Bejan. On the boundary layer regime in a vertical enclosure filled with a porous medium. *Letters in Heat and Mass Transfer*, 6(2):93–102, Mar. 1979. ISSN 0094-4548. doi: 10.1016/0094-4548(79)90001-8. URL https://www.sciencedirect.com/science/article/pii/0094454879900018.

[7] J. Belabid, S. Belhouideg, K. Allali, O. Mahian, and E. Abu-Nada. Numerical simulation for impact of copper/water nanofluid on thermo-convective instabilities in a horizontal porous annulus. *Journal of Thermal Analysis and Calorimetry*, 138(2):1515–1525, Oct. 2019. ISSN 1588-2926. doi: 10.1007/s10973-019-08265-x. URL https://doi.org/10.1007/s10973-019-08265-x.

[8] M. Ghalambaz, M. A. Sheremet, and I. Pop. Free Convection in a Parallelogrammic Porous Cavity Filled with a Nanofluid Using Tiwari and Das' Nanofluid Model. *PLOS ONE*, 10(5):e0126486, May 2015. ISSN 1932-6203. doi: 10.1371/journal.pone.0126486. URL https://dx.plos.org/10.1371/journal.pone.0126486.

[9] R. J. Gross, M. R. Baer, and J. C. E. Hickox. The application of flux-corrected transport (fct) to high rayleigh number natural convection in a porous meduim. Begel House Inc., 1986. doi: 10.1615/IHTC8.3820. URL https://www.ihtcdigitallibrary.com/conferences/57dcad5042ab3940,00cc1ddb0a7a01be,495dcb5c29b8d4f0.html.

[10] Z. Haddad, H. F. Oztop, E. Abu-Nada, and A. Mataoui. A review on natural convective heat transfer of nanofluids. *Renewable and Sustainable Energy Reviews*, 16(7):5363–5378, Sept. 2012. ISSN 1364-0321. doi: 10.1016/j.rser.2012.04.003. URL https://www.sciencedirect.com/science/article/pii/S1364032112002602.

[11] S. Y. Jung and H. Park. Experimental investigation of heat transfer of Al2O3 nanofluid in a microchannel heat sink. *International Journal of Heat and Mass Transfer*, 179:121729, Nov. 2021. ISSN 0017-9310. doi: 10.1016/j.ijheatmasstransfer.2021.121729. URL https://www.sciencedirect.com/science/article/pii/S0017931021008358.

[12] P. Keblinski, J. A. Eastman, and D. G. Cahill. Nanofluids for thermal transport. *Materials Today*, 8(6):36–44, June 2005. ISSN 1369-7021. doi: 10.1016/S1369-7021(05)70936-6. URL https://www.sciencedirect.com/science/article/pii/S1369702105709366.

[13] D. Manole and J. Lage. Numerical benchmark results for natural convection in a porous medium cavity. In *Heat and Mass Transfer in Porous Media, ASME Conference 1992*, volume 216, pages 55–60, 1992.

[14] D. A. Nield and A. Bejan. *Convection in Porous Media*. Springer International Publishing, Cham, 2017. doi: 10.1007/978-3-319-49562-0.

[15] H. F. Oztop and E. Abu-Nada. Numerical study of natural convection in partially heated rectangular enclosures filled with nanofluids. *International Journal of Heat and Fluid Flow*, 29(5):1326–1336, Oct. 2008. ISSN 0142-727X. doi: 10.1016/j.ijheatfluidflow.2008.04.009. URL https://www.sciencedirect.com/science/article/pii/S0142727X08000933.

[16] A. Rahimi, A. Dehghan Saee, A. Kasaeipoor, and E. Hasani Malekshah. A comprehensive review on natural convection flow and heat transfer: The most practical geometries for engineering applications. *International Journal of Numerical Methods for Heat & Fluid Flow*, 29(3):834–877, Jan. 2018. ISSN 0961-5539. doi: 10.1108/HFF-06-2018-0272. URL https://doi.org/10.1108/HFF-06-2018-0272. Publisher: Emerald Publishing Limited.

[17] P. Rao and P. Barman. Natural convection in a wavy porous cavity subjected to a partial heat source. *International Communications in Heat and Mass Transfer*, 120:105007, Jan. 2021. ISSN 07351933. doi: 10.1016/j.icheatmasstransfer.2020.105007. URL https://linkinghub.elsevier.com/retrieve/pii/S0735193320305352.

[18] F. Redouane, W. Jamshed, S. S. U. Devi, M. Prakash, N. A. A. M. Nasir, Z. Hammouch, M. R. Eid, K. S. Nisar, A. B. Mahammed, A.-H. Abdel-Aty, I. S. Yahia, and E. M. Eed. Heat flow saturate of Ag/MgO-water hybrid nanofluid in heated trigonal enclosure with rotate cylindrical cavity by using Galerkin finite element. *Scientific Reports*, 12(1):2302, Feb. 2022. ISSN 2045-2322. doi: 10.1038/s41598-022-06134-6. URL https://www.nature.com/articles/s41598-022-06134-6. Number: 1 Publisher: Nature Publishing Group.

[19] M. S. Sadeghi, N. Anadalibkhah, R. Ghasemiasl, T. Armaghani, A. S. Dogonchi, A. J. Chamkha, H. Ali, and A. Asadi. On the natural convection of nanofluids in diverse shapes of enclosures: an exhaustive review. *Journal of Thermal Analysis and Calorimetry*, 147(1):1–22, Jan. 2022. ISSN 1588-2926. doi: 10.1007/s10973-020-10222-y. URL https://doi.org/10.1007/s10973-020-10222-y.

[20] M. Sharifpur, A. B. Solomon, T. L. Ottermann, and J. P. Meyer. Optimum concentration of nanofluids for heat transfer enhancement under cavity flow natural convection with TiO2 – Water. *International Communications in Heat and Mass Transfer*, 98:297–303, Nov. 2018. ISSN 0735-1933. doi: 10.1016/j.icheatmasstransfer.2018.09.010. URL https://www.sciencedirect.com/science/article/pii/S073519331830229X.

[21] M. A. Sheremet, T. Grosan, and I. Pop. Free Convection in a Square Cavity Filled with a Porous Medium Saturated by Nanofluid Using Tiwari and Das' Nanofluid Model. *Transport in Porous Media*, 106(3):595–610, Feb. 2015. ISSN 0169-3913, 1573-1634. doi: 10.1007/s11242-014-0415-3. URL http://link.springer.com/10.1007/s11242-014-0415-3.

[22] S. Sivasankaran, H. T. Cheong, and M. Bhuvaneswari. Natural convection in an inclined porous triangular enclosure with various thermal boundary conditions. *Thermal Science*, 23(2 Part A):537–548, 2019. URL https://www.doiserbia.nb.rs/Article.aspx?id=0354-98361800159S.

[23] Q. Sun and I. Pop. Free convection in a tilted triangle porous cavity filled with cu-water nanofluid with flush mounted heater on the wall. *International Journal of Numerical Methods for Heat & Fluid Flow*, 24(1):2–20, Jan. 2014. ISSN 0961-5539. doi: 10.1108/HFF-10-2011-0226. URL https://doi.org/10.1108/HFF-10-2011-0226. Publisher: Emerald Group Publishing Limited.

[24] R. K. Tiwari and M. K. Das. Heat transfer augmentation in a two-sided lid-driven differentially heated square cavity utilizing nanofluids. *International Journal of Heat and Mass Transfer*, 50(9):2002–2018, May 2007. ISSN 0017-9310. doi: 10.1016/j.ijheatmasstransfer.2006.09.034. URL https://www.sciencedirect.com/science/article/pii/S001793100600576X.

[25] K. Vafai. *Handbook of Porous Media*. CRC Press, 2005.

[26] L. Xu, A. Khalifeh, A. Khandakar, and B. Vaferi. Numerical investigating the effect of Al2O3-water nanofluids on the thermal efficiency of flat plate solar collectors. *Energy Reports*, 8:6530–6542, Nov. 2022. ISSN 2352-4847. doi: 10.1016/j.egyr.2022.05.012. URL https://www.sciencedirect.com/science/article/pii/S2352484722008599.

[27] S. Yao, T. Huang, J. Zeng, L. Duan, and K. Zhao. The study of natural convection heat transfer of nanofluids in a partially porous cavity based on Lattice Boltzmann Method. *Thermal Science*, 23 (2 Part B):1003–1015, 2019. URL https://www.doiserbia.nb.rs/Article.aspx?ID=0354-98361700169S.